1972

# Further experiments with an hurricane-ocean interaction model.

Pearson, Nils Alexander Silliman.

Monterey, California. Naval Postgraduate School

# FURTHER EXPERIMENTS WITH AN HURRICANE-OCEAN INTERACTION MODEL

Nils Alexander Silliman Pearson

# NAVAL POSTGRADUATE SCHOOL
## Monterey, California

# THESIS

Further Experiments with an Hurricane-

Ocean Interaction Model

by

Nils Alexander Silliman Pearson

Thesis Advisor: R. L. Elsberry

September 1972

# Further Experiments with an Hurricane-
# Ocean Interaction Model

by

Nils Alexander Silliman Pearson
Lieutenant Commander, United States Navy
B.S., United States Naval Academy, 1964

Submitted in partial fulfillment of the
requirements for the degree of

MASTER OF SCIENCE IN METEOROLOGY

from the

NAVAL POSTGRADUATE SCHOOL
September 1972

ABSTRACT

Modifications were made to Corgnati's (1971) steady state, symmetrical hurricane model, which was based on a model proposed by Riehl (1963), and in which bulk aerodynamic transfer formulas were used to predict the air-sea interaction below a specified vortex. The modifications resulted in a more flexible model in which hurricane intensity was controlled by sensible and latent heat fluxes, which were in turn dependent on the ocean surface temperature. A boundary layer model based on similarity theory was then used, to specify air-sea interaction, by replacing the bulk transfer formulas with Cardone's (1969) extension of Blackadar's (1965) two-layer neutral, baroclinic boundary layer model. To achieve realistic results the time scale was modified to include centripetal acceleration, which resulted in a decreasing height of frictional influence with decreasing radius. Varying Cardone's formulation of roughness length and the ratio of eddy exchange coefficients for heat and moisture resulted in stress and heat flux values in agreement with values determined from hurricane observations. Including the complete boundary layer model resulted in greater sensitivity to ocean temperature variations than when bulk transfer formulas were used to determine the air-sea interaction.

TABLE OF CONTENTS

LIST OF FIGURES

LIST OF TABLES

LIST OF SYMBOLS

| | |
|---|---|
| $a_h$ | Reciprocal of the turbulent Prandtl number ($K_h/K_m$) |
| $\alpha$ | Cross isobar angle of surface gradient wind |
| $B_o$ | Blackadar constant = 0.81 |
| $C_D$ | Drag coefficient |
| $C_p$ | Specific heat of air at constant pressure |
| $C_z$ | Drag coefficient at level z |
| $e_s$ | Saturation vapor pressure |
| f | Coriolis parameter |
| f' | Reciprocal of time scale ($f + V_\theta R^{-1}$) |
| G | Gravity = 9.8 meters/second |
| H | Upward turbulent heat flux |
| h | Height of the surface layer |
| $K_h$ | Turbulent transfer coefficient for heat |
| $K_m$ | Turbulent transfer coefficient for momentum |
| k | von Kármán constant = .35 |
| L | Lettau-Monin-Obukhov stability length |
| L' | Modified stability length |
| $L_v$ | Latent heat of vaporization of water |
| P | Pressure |
| $Q_e$ | Latent heat release rate |
| $Q_s$ | Sensible heat transfer rate |
| $q_a$ | Specific humidity at $T_a$ |
| $q_w$ | Saturated specific humidity at $T_w$ |
| $\phi_t$ | Nondimensional temperature gradient |
| $\phi_u$ | Nondimensional wind shear |

| | |
|---|---|
| $\psi$ | Integrated profile stability parameter |
| $R$ | Radial distance from center of hurricane |
| $R_i$ | Radius of maximum $V_\theta$ |
| $R_o$ | Radius where $V_\theta$ is equal to zero in the outflow |
| $Ro$ | Surface Rossby number |
| $\rho$ | Mean density of surface boundary layer |
| $T_a$ | Atmospheric temperature |
| $T_{ae}$ | Pseudo-equivalent temperature |
| $T_w$ | Ocean surface temperature |
| $\theta$ | Angular measure |
| $\theta_*$ | Scaling temperature |
| $\theta_a$ | Potential temperature |
| $\theta_e$ | Equivalent potential temperature |
| $\theta_{e_i}$ | Equivalent potential temperature at $R_i$ |
| $\theta_{e_o}$ | Equivalent potential temperature at $R_o$ |
| $\tau$ | Surface stress |
| $U_*$ | Friction velocity |
| $U_z$ | Wind at height z |
| $V$ | Estimated surface wind |
| $V_r$ | Radial wind component |
| $V_g$ | Gradient wind |
| $V_\theta$ | Tangential wind component |
| $V_{\theta_i}$ | Maximum tangential wind component |
| $\omega$ | Vertical velocity in pressure coordinates |
| $z$ | Height above sea level |
| $z_o$ | Surface roughness parameter |

## ACKNOWLEDGEMENT

The author wishes to express his sincere gratitude to Dr. R. L. Elsberry for the many hours he willingly spent guiding me in this work, and Dr. K. L. Davidson for his guidance during Dr. Elsberry's absence and his aid in the interpretation of similarity theory.

An earlier thesis by McConathy (1972) proved invaluable in applying and interpreting the results obtained from the boundary layer model based on similarity theory.

# I. INTRODUCTION

It is well recognized that sea surface temperature affects hurricane intensity; the hurricane winds in turn, exert a stress on the ocean surface and induce the extraction of heat and moisture. A "steady state" hurricane model requires that a balance exists in this energy exchange between air and ocean.

Riehl (1963) described a two-layer model for an axisymmetric hurricane in which a balance existed between the heat source and momentum sink at the air-sea interface. The "steady state" upper level vortex was then specified based on the air-sea interaction within the boundary layer.

Corgnati (1971) used Riehl's model to construct a numerical model which used predictive equations for heat and moisture within the boundary layer, and bulk transfer formulas for fluxes at the air-sea interface. It was felt that considerable improvement in Corgnati's model could be attained through the use of recent boundary layer models based on Monin-Obuhkov "similarity theory"; specifically through the use of Cardone's (1969) extension of Blackadar's (1965) two-layer neutral baroclinic boundary layer model.

The purpose of this study was to modify Corgnati's numerical model so as to better define the air-sea interaction.

Several numerical simulations of hurricane development have been made with complicated multi-level models. These models include some interaction with the ocean. The scope of this study was to model only the boundary layer beneath an upper level vortex, defined by Riehl's model, which responds to the air-sea interaction.

# II. DISCUSSION OF THE MODEL

## A. REVIEW OF RIEHL'S MODEL

Riehl's two-layer model consisted of an inflow layer and an outflow layer (Figure 1). Riehl and Malkus (1961) have shown the conservation of absolute angular momentum is a reasonable first approximation in the outflow layer. This constraint leads to the expression for computing the radius at which the tangential component of the outflow goes from cyclonic to anticyclonic,

$$R_o = (2\, V_{\theta_i}\, R_i/f)^{1/2} , \tag{1}$$

where $R_i$ is the eye wall radius and $V_{\theta_i}$ is the tangential wind at $R_i$.

Riehl and Malkus (1961) also demonstrated the approximate conservation of potential vorticity in the inflow layer. Riehl (1963) applied this to the equation of motion in polar coordinates (see Figure 2)

$$\frac{dV_\theta}{dt} + \frac{V_\theta V_r}{R} + fV_r = -\frac{1}{\rho}\,\frac{\partial P}{R\partial\theta} + \frac{1}{\rho}\,\frac{\partial \tau_\theta}{\partial z} , \tag{2}$$

and integrated over the depth of the inflow layer to get

$$R\tau_\theta = \text{constant} , \tag{3}$$

where $\tau_\theta$ is the tangential surface stress. Using the expression

$$\tau_\theta = C_D\, \rho_s\, V^2_{\theta_s} / \cos\alpha , \tag{4}$$

and assuming the drag coefficient ($C_D$) and surface density ($\rho_s$) to be constant, also that the inflow angle is small enough so that cosine $\alpha$ can be closely approximated by unit yields the expression

$$V_\theta\, R^{1/2} = \text{constant} . \tag{5}$$

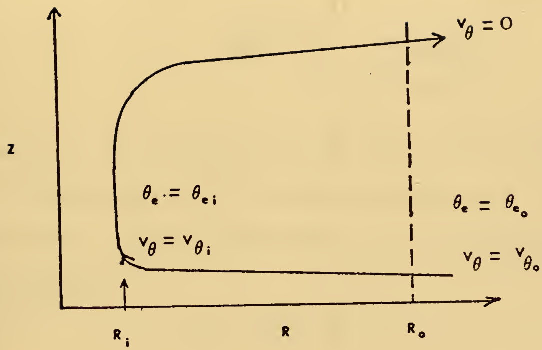


Figure 1. Illustrating hurricane mass circulation $V_\theta$ is tangential wind component, $\theta_e$ is equivalent potential temperature, R is radius.

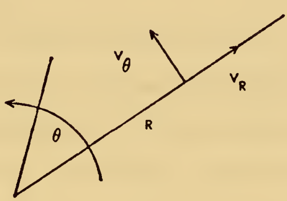


Figure 2. Illustrating polar coordinate system used, $V_\theta$ is tangential wind component, $V_r$ is radial wind component, R is radius, $\theta$ is angular measurement.

Riehl (1963) and Shea (1972) have shown this to be a reasonably good approximation to the $V_\theta$-R profiles.

Equation (2) can also be solved for the radial wind profile,

$$V_r = - \frac{GC_D \rho V_\theta^2}{\Delta P} \left( \frac{1}{f + \frac{V_\theta}{R} + \frac{\partial V_\theta}{\partial R}} \right) , \qquad (6)$$

where G is the acceleration of gravity, and f is the coriolis parameter.

Integration of the hydrostatic equation, for typical values of equivalent potential temperature ($\theta_e$) in a hurricane, produces the relationship

$$P' = - 2.56 \; \theta'_e \quad , \qquad (7)$$

where P' is the pressure departure from 1005 mb and $\theta'_e$ is the departure from 350K. Riehl (1963) also determined a relation between the maximum tangential wind ($V_{\theta_i}$) and the equivalent potential temperature ($\theta_{e_i}$) at the eye wall by equating $V_{\theta_i}$ to the height gradient of the isobaric surfaces and applying a cyclostrophic relationship to obtain

$$V_{\theta_i} \text{ (m/sec)} = 14.1(\theta_{e_i} - \theta_{e_o})^{1/2} , \qquad (8)$$

where subscript "o" denoted the value at $R_o$.

From these equations it can be seen that the upper level vortex is dependent on the increase in $\theta_e$ in the boundary layer. The problem becomes one of modeling the boundary layer air-sea interaction so that the $\theta_e$ increase corresponds to the upper level vortex.

## B. CORGNATI'S MODEL

### 1. Prediction Equation

#### a. Atmospheric Prediction

In the atmosphere the predicted variables were heat and moisture in the form of potential temperature ($\theta_a$) and specific humidity ($q_a$) respectively. These two parameters, along with pressure (P), determined $\theta_e$ which was the one factor in determining the maximum wind (Equation 8).

Partial derivatives were approximated using finite differencing techniques to solve the thermodynamic equation in the following form

$$\frac{\partial \theta_a}{\partial t} = -\left[\frac{\partial V_\theta \theta_a}{R\partial\theta} + \frac{\partial V_r R\theta_a}{R\partial R}\right] + \frac{\partial\omega\theta_a}{\partial P} + \frac{Q_s G}{C_p \Delta P} , \qquad (9)$$

where $\omega$ is the vertical motion and $Q_s$ is sensible heat transfer. The first term on the right hand side was neglected due to symmetry. The boundary layer was assumed well mixed with height, and therefore, $\theta_a$ could be calculated from the surface values of air temperature and pressure. Moisture changes were determined in a similar fashion using the expression

$$\frac{\partial q_a}{\partial t} = -\left[\frac{\partial V_\theta q_a}{R\partial\theta} + \frac{\partial V_r R q_a}{R\partial R} + \frac{\partial\omega q_a}{\partial P}\right] + \frac{Q_e G}{L\Delta P} , \qquad (10)$$

where $Q_e$ is the latent heat transfer.

Corgnati (1971) used bulk aerodynamic transfer formulas for determining the transfer of latent and sensible heat in the form

$$Q_s = \frac{2}{3} C_p \rho_s C_D (T_w - T_a) V , \qquad (11)$$

$$Q_e = \frac{2}{3} L_v \rho_s C_D (q_w - q_a) V , \qquad (12)$$

where $C_p$ is the specific heat of dry air, $L_v$ is the latent heat of vaporization of water, $\rho_s$ is the atmospheric density at the sea surface, $T_w - T_a$ is the air-sea temperature difference, $q_a$ and $q_w$ are the

specific humidity of the air and the saturated specific humidity at the sea surface temperature. The surface wind (V) was approximated at 70% of the wind at the top of the boundary layer (Equation 5). Furthermore, Robinson's (1966) heat transfer coefficient (2/3 $C_D$) was used, which takes molecular processes near the surface into account.

Vertical motion at the top of the boundary layer was computed from the continuity equation in polar coordinates,

$$\frac{\partial V_\theta}{R\partial\theta} + \frac{\partial RV_r}{R\partial R} + \frac{\partial\omega}{\partial p} = 0 \tag{13}$$

where the first term is zero due to symmetry. Vertical motion at the surface was assumed to be zero, and a boundary layer 100 mb thick was used, based on the assumption that effects within the boundary layer would not exceed this height.

b. Oceanic Prediction

Predicted variables in the oceanic portion of Corgnati's model were sea surface temperature ($T_w$) and the saturated specific humidity at the sea surface temperature. A temperature gradient of 2C per 100 meters with a layer depth of 100 meters described the ocean structure. The amount of heat removed, through latent and sensible heat transfer, was computed and the temperature of the ocean surface reduced accordingly. Corgnati found that, since the model was stationary, reductions in $T_w$ led to reduced air-sea transfers and, therefore, reduced wind speed. In order to test only the atmospheric portion of the model the sea temperature was fixed.

2. Initialization of Surface Temperatures and Humidities

The relationship between $\theta_{e_i}$, tangential wind at the eye wall ($V_{\theta_i}$), and pressure at the eye wall ($P_i$) made it possible, by specifying

$V_{\theta_i}$, to solve for $\theta_{e_i}$ and $P_i$ using Equations (7) and (8). The surface pressure distribution was then determined by assuming a gradient wind balance.

Initialization of the temperature and moisture fields, both in the boundary layer and at the ocean surface, were important parts of the model. The surface water temperature was set at 30C, then the available moisture at the ocean surface was calculated from the integrated form of Clapeyron's equation

$$\mathrm{Ln}\,\frac{e_s}{6.105} = 25\,\frac{T-273}{T} - 5.2\,\mathrm{Ln}\,\frac{T}{273}\,, \tag{14}$$

where $e_s$ is the saturated vapor pressure. Air in contact with the water was assumed saturated, with the specific humidity calculated from

$$q_w = \frac{.622\,e_s}{P - .373e_s}\;. \tag{15}$$

The equivalent potential temperature was computed by applying the relationship between height gradient of the isobaric surfaces and the tangential wind field.

By specifying the initial state from the equivalent potential temperature at the eye wall, the effect of expansion cooling and sensible heat source at the surface were taken into account. Riehl (1963) suggested that $\theta_e$ must rise above 350-352K to allow deep convection, which warms the column and lowers the central pressure to values which can sustain hurricane force winds.

Specific humidity of the air ($q_a$) was calculated assuming the initial air temperature ($T_a$) equal to the water temperature, from

$$q_a = T_a\,\frac{C_p}{L_v}\,\mathrm{Ln}\,\frac{T_{ae}}{T_a}\;, \tag{16}$$

where $T_{ae}$ is the pseudo-equivalent air temperature.

## C. MODIFICATIONS TO CORGNATI'S NUMERICAL MODEL

Corgnati (1971) used a 17 by 17 rectangular grid with 15 nautical mile spacing. The center of the grid was the hurricane center, and variables were computed along a diagonal and interpolated to the other grid points. Due to the symmetry of the model, the four quadrants had identical results, and as much information could be derived through the use of a one-dimensional model. Resolution was increased by using 100 grid points spaced at 3 kilometer intervals along a radial. One disadvantage of the increased resolution was that smaller time steps had to be used, although this was partially compensated by the reduction in the number of grid points. Inherent instability in a forward-in-time, centered-in-space finite differencing technique, made it necessary to change to a leapfrog technique with a forward time step every 24 time steps.

The equivalent potential temperature gradient was the determining factor in predicting the maximum wind. When deriving Equation (8), Riehl assumed cyclostrophic flow, so that the relationship was only a good approximation in the area of maximum winds. Assuming gradient winds led to the relationship

$$\frac{V_\theta^2}{R} + fV_\theta = -\frac{2.5 \times 10^3}{\rho}\frac{\partial\theta_e}{\partial R}\ , \qquad (17)$$

which was used during the initialization to determine the equivalent potential temperature field.

The interdependence of the equivalent potential temperature field and the wind field makes the selection of the eye wall and outer radii important factors in determining the wind field. The inner radius was allowed to adjust towards the radius of maximum equivalent potential

temperature, rather than remain fixed as in Corgnati's model, and the outer radius was determined from Equation (1). The maximum tangential wind component was then determined from Equation (17) using the gradient of equivalent potential temperature from the eye wall to the outer radius.

Corgnati (1971) found that relative humidity values at the eye wall region exceeded saturated conditions after a short period of time. He theorized that cumulus clouds, in the form of "hot towers", with the moist ascending air being replaced by relatively dry subsiding air, would serve to remove this excessive moisture. To model the "hot towers" Corgnati removed all moisture in excess of a critical value of 95% relative humidity, and measured this as convective precipitation. A similar problem was encountered at the outer radius, where the computed value of $\theta_e$ was found to be significantly higher than the 350K specified by Riehl. Since the maximum wind was dependent on the radial gradient of $\theta_e$, the increased $\theta_e$ caused a decrease in the wind field. To correct this, a critical relative humidity of 75% was used at the outer radius. This simulated the relatively dry subsiding air outside a hurricane. Several profiles of critical relative humidity were experimented with and will be discussed later.

Corgnati (1971) experimented with the release of latent heat, within the boundary layer, of the excess moisture removed through cumulus convection. Releasing all the latent heat within the boundary layer greatly increased the hurricane intensity. The bases of cumulus clouds within hurricanes have been observed to be lower towards the eye. To model this, latent heat release was made an inverse function of radial distance.

With these changes it was now possible, through latent heat release, relative humidity control and ocean temperature adjustments, to model steady state hurricanes of different intensities.

## D. CARDONE'S BOUNDARY LAYER MODEL

The use of bulk aerodynamic transfer formulas requires some knowledge of heat and moisture exchange coefficients as well as winds within the surface layer. Recent advances in the study of atmospheric turbulence have led to a greater confidence in describing the distribution of wind and temperature in the atmospheric boundary layer. This progress has arisen largely through the application of the Monin-Obuhkov "similarity theory", which has been supported by observational studies. Cardone (1969) has extended Blackadar's (1965) two-layer, neutral, baroclinic boundary layer model, over fixed terrain, to the boundary layer over the sea. McConathy (1972) evaluated Cardone's formulation of the marine boundary layer. The results of McConathy's study were used to apply Cardone's specification of the boundary layer, instead of the bulk aerodynamic transfer formulas in Corgnati's model, and to determine a radial wind profile throughout the boundary layer.

The Monin-Obuhkov "similarity theory" for the constant stress, or surface layer, predicts that a universal relation should exist for the wind shear,

$$\frac{\partial u}{\partial z} = \frac{U_*}{kz} \phi_u \quad , \tag{18}$$

and the temperature gradient,

$$\frac{\partial \theta_a}{\partial z} = \frac{\theta_*}{z} \phi_t \quad , \tag{19}$$

where the friction velocity ($U_*$) is defined as

$$U_* = \left(\frac{\tau}{\rho}\right)^{1/2} \quad , \tag{20}$$

and the scaling temperature

$$\theta_* = \frac{1}{kU_*} \quad \frac{H}{C_p \rho} \quad , \tag{21}$$

k is von Karman's constant of .35, z is the height, H is the total heat flux, $\phi_u$ and $\phi_t$ are functions of stability. Matching the integrated equations for the Ekman layer to the integrated equation for the constant stress layer at top of the surface layer led to the following set of equations, in terms of $U_*$ and inflow angle ($\alpha$),

$$\frac{U_*}{V_g} = [2kB_o \sin^2\alpha \; \phi_u \; (\frac{h}{L'})]^{1/2} \quad , \tag{22}$$

and

$$\frac{U_*}{V_g} = \frac{k\sqrt{2} \sin (\frac{\pi}{4} - \alpha)}{\mathrm{Ln}B_o\mathrm{Ro} - \psi(h/L')} \quad , \tag{23}$$

where the integrated profile stability parameter is defined by

$$\psi = 1 - \phi_u - 3\mathrm{Ln}\phi_u + 2\mathrm{Ln}(\frac{1+\phi_u}{2}) + 2 \tan^{-1}\phi_u - \frac{\pi}{2} + \mathrm{Ln}(\frac{1+\phi_u^2}{2}) \quad , \tag{24}$$

and the height of the surface layer (h) is defined by

$$h = \frac{B_o V_g}{f} \quad , \tag{25}$$

the surface Rossby number (Lettau 1959) by

$$\mathrm{Ro} = \frac{V_g}{fZ_o} \quad , \tag{26}$$

and the modified stability length (Panofsky 1963) by

$$L' = \frac{K_h}{K_m} \quad L = \frac{U_* T \; \partial u/\partial z}{kG \; \partial\theta/\partial z} \quad . \tag{27}$$

In these expressions $V_g$ is the surface geostrophic wind, and $B_o$ is Blackadar's constant of 0.0003. The drag coefficient ($C_z$) was defined in terms of the roughness parameter ($Z_o$) and stability parameter as

$$C_z = \left[\frac{k}{L_n \; z/Z_o - \psi(z/L')}\right]^2 \quad . \tag{28}$$

The roughness parameter was formulated by Cardone (1969) as

$$Z_o = \frac{6.84 \times 10^{-5}}{U_*} + 4.28 \times 10^{-3} U_*^2 - 4.43 \times 10^{-4} \qquad (29)$$

where the second term on the right hand side represents Charnock's(1955) formulation for aerodynamically rough flow under high wind speed conditions,

$$Z_o = \frac{.035 U_*^2}{G} \quad . \qquad (30)$$

Equations (22) and (23) were solved simultaneously for $U_*/V_g$ and $\alpha$ from the external parameters $V_g$, f, and air-sea virtual temperature difference.

E. APPLICATION OF CARDONE'S BOUNDARY LAYER MODEL

Cardone's model was applied to the balanced hurricane to determine the fluxes of heat and moisture as well as momentum transfer. The determination of a mean radial wind component, using Cardone's model, assured continuity in determining advection within the boundary layer.

The tangential wind, which represented a gradient wind at the top of the boundary layer, was corrected for thermal wind and used as the surface gradient wind.

To include the centripetal acceleration, the coriolis parameter was replaced by

$$f' = f + \frac{V_\theta}{R} \quad . \qquad (31)$$

By assuming the turbulent transfer coefficient for heat ($K_h$) equals the turbulent transfer coefficient for momentum ($K_m$), and knowing L'from the solution of Equations (22) and (23), the total heat transfer was determined using

$$L' \frac{K_m}{K_h} = L = - \frac{U_*^3 C_p \rho_a T}{kGH} \quad . \qquad (32)$$

The total heat (H) was then separated into latent and sensible components by assuming their ratio was determined by

$$\frac{Q_s}{Q_e} = \frac{C_p}{L_v}\left(\frac{\theta_a - \theta_w}{q_a - q_w}\right) \tag{33}$$

The predictive Equations (9) and (10) required a radial wind for advecting the heat and moisture. The assumption that heat and moisture are homogeneous, within the depth of the boundary layer, made it possible to use an integrated value of radial wind. This was determined by solving the integrated form of Equation (18)

$$U_z = \frac{U_*}{k}\left[L_n \frac{z}{Z_o} - \psi\left(\frac{z}{L'}\right)\right] \quad , \tag{34}$$

at $z = \frac{h}{i}$ $i = 1, 2, 3, 4$, and averaging these values. The mean radial wind in the surface layer was then determined by multiplying by the sine of the inflow angle ($\alpha$). The inflow within the spiral layer was determined through integration of the Ekman solution through the spiral layer to get

$$\int_h^\infty V_r dz = \sqrt{2}\, V_\theta \sin\alpha \, \frac{e^{-Bh}}{2Bh}\left[\cos\left(\alpha + \frac{3\pi}{4} - Bh\right) - \sin\left(\alpha + \frac{3\pi}{4} - Bh\right)\right], \tag{35}$$

where

$$B = \left(\frac{f}{2U_* kh}\right)^{1/2} \tag{36}$$

The two integrated values of $V_r$ from Equations (34) and (35) were then used in determining the vertical motion (Equation 13), and the advection of heat and moisture (Equations 9 and 10) in the predictive portion of the model.

# III. DISCUSSION OF RESULTS

The numerical process encompassed three stages. First was an initialization phase in which the model was started with a given $V_e$, $T_w$, $T_a$, and $R_i$, then the model went through an adjustment process in which the moisture content in the boundary layer increased until either a balance was reached between latent heat flux and moisture advection, or the moisture reached the critical relative humidity values. The final stage was a "steady state" in which the time variations of heat and moisture in the boundary layer were small.

The following discussion deals with the interpretation of results obtained when various parameters were changed, both in the initial and adjustment stages of the model. Due to the complex interactions of the model, a simplistic approach of establishing a base run and then varying one parameter at a time was used. This type of experimentation made the effects of the changes more obvious.

## A. CORGNATI'S MODIFIED MODEL

The modifications to Corgnati's model, as discussed in the previous section, were incorporated to achieve more flexibility in describing hurricanes of varying intensity. Corgnati discussed in detail the adjustment process. He found that steady state was dependent on latent heat release and critical relative humidity used to simulate the cumulus convection. These parameters control, to a good part, the heat and moisture at the eye wall ($R_i$), which in turn determines the equivalent potential temperature ($\theta_{e_i}$) and, therefore, the hurricane intensity (Equation 8).

The parameters varied were initial air temperature, water temperature, critical relative humidity, and latent heat release within the boundary layer. Figures 3 through 15 illustrate the relationships between the various parameters, and were obtained from the base run with water temperature set at 30C, air temperature initialized at 29C, critical relative humidity set at 95% at $R_i$, with a linear profile to 75% at $R_o$, and no latent heat release within the boundary layer.

Air temperature (Figure 3) exhibited a nearly isothermal (less than .3C) profile from $R_o$ to about $3R_i$, with an approximately logarithmic drop from $3R_i$ to a minimum temperature at $R_i$. The temperature drop corresponds to the very strong horizontal pressure gradient (Figure 4). The adiabatic cooling due to expansion would cause about a 5 C drop, but, as Riehl (1954) pointed out, the blowing spray in the high wind region would greatly increase the effective surface area and, therefore, the latent and sensible heat transfer. This enhanced transfer would offset the adiabatic cooling and account for the slight temperature decrease towards the eye as observed by Deppermann (1939). The bulk transfer formulas (Equations 11 and 12) do not take into account the enhanced transfer due to the blowing spray. However, the increased wind speed and air-sea temperature difference were sufficient to increase the sensible and latent heat fluxes and offset much of the adiabatic cooling.

Relative humidity (Figure 5) was at the critical value which indicates the steady state stage was one in which the flux and advection of moisture was kept in balance through the removal of moisture exceeding the critical relative humidity. Figure 15 indicates the moisture removed to keep the relative humidity at the critical value.

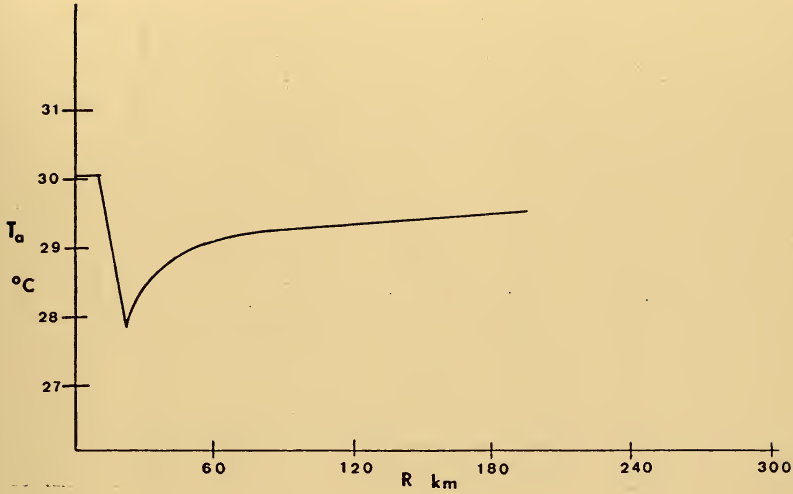


Figure 3. Radial profile of air temperature for the base run of Corgnati's modified model, $T_w$ = 30C, $T_a$ initialized at 29C.

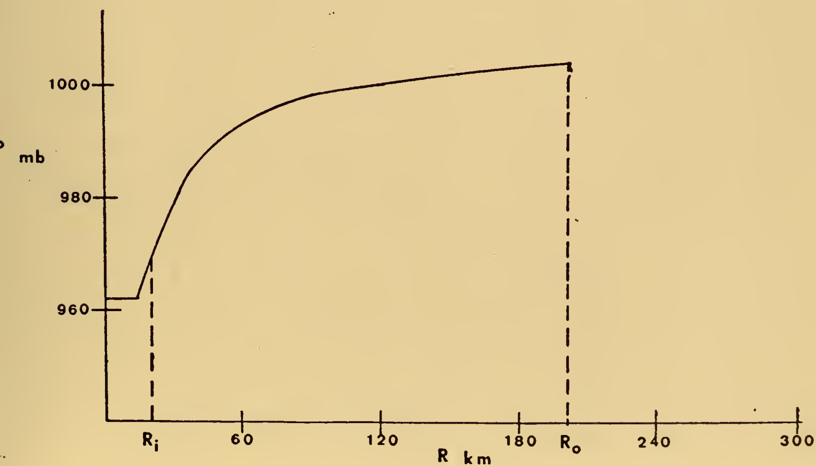


Figure 4. Same as Figure 3 except pressure.

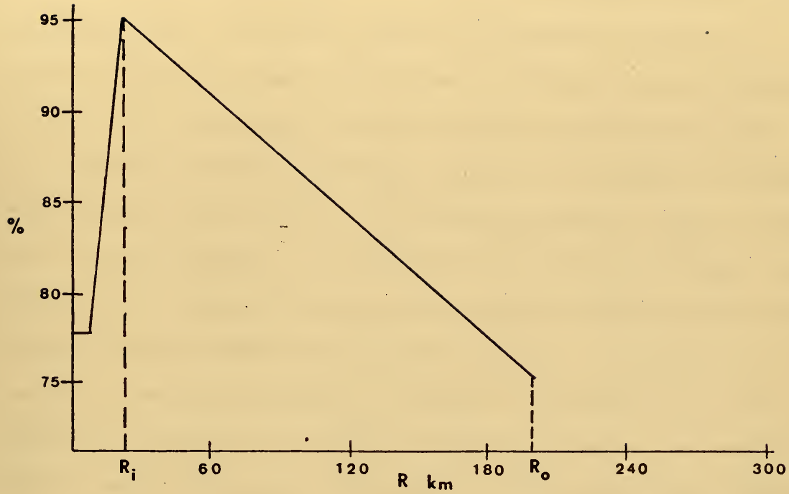


Figure 5. Same as Figure 3 except relative humidity.

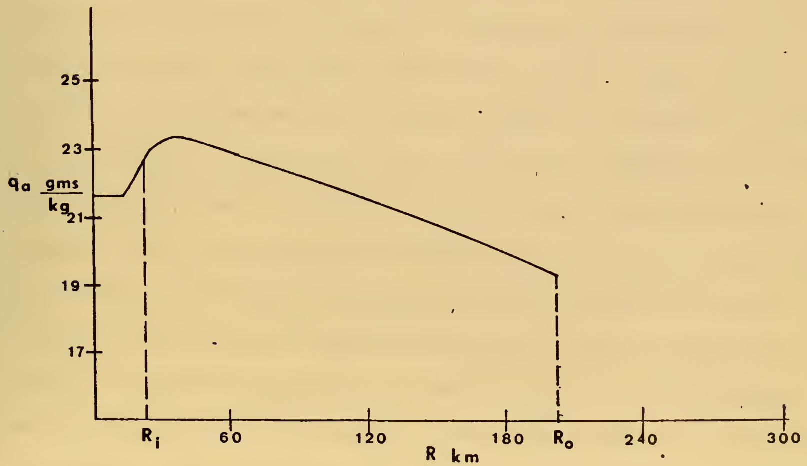


Figure 6. Same as Figure 3 except specific humidity.

Specific humidity (Figure 6) followed the relative humidity in the isothermal region. The sharp decrease in temperature reduced the amount of moisture, despite the increase in critical relative humidity, and the result was a peak in specific humidity outside the eye wall.

Equivalent potential temperature (Figure 7) is dependent on temperature, moisture, and pressure. In the nearly isothermal region and with small pressure gradient, $\theta_e$ is governed by the amount of moisture. From $3R_i$ to $R_i$ the temperature decrease has a two-fold effect in that it also reduces specific humidity and $\theta_e$ becomes linear. The gradient of $\theta_e$ between $R_i$ and $R_o$ determines $V_{\theta_i}$ (Equation 17), and Equation (5) describes the tangential wind profile (Figure 8). Pressure and wind are linked through the gradient wind equation, and the sharp wind increase is reflected by the strong pressure gradient.

In a hurricane the winds rotating about the eye experience both centripetal and coriolis acceleration (Figure 9). In the outer portion of the hurricane coriolis dominates. However, as $V_\theta$ increases and radius decreases, centrifugal force becomes dominant, supporting the strong pressure gradient in the eye wall regions, and causing a decrease in integrated $V_r$. The decrease in $V_\theta$ in the near surface region requires cross isobaric flow; this results in a frictional force opposing the pressure force. The importance of these various forces and their region of influence will become more apparent in the discussion of results obtained using Cardone's boundary layer model. Figure 10 shows the effect of cyclostrophic flow on the radial wind. The strong vertical motion (Figure 11) at the eye wall is due to the decrease in radial wind towards the eye wall and the decreasing circumference (Equation 13). In reality the vertical motion is due to deep convection maintained

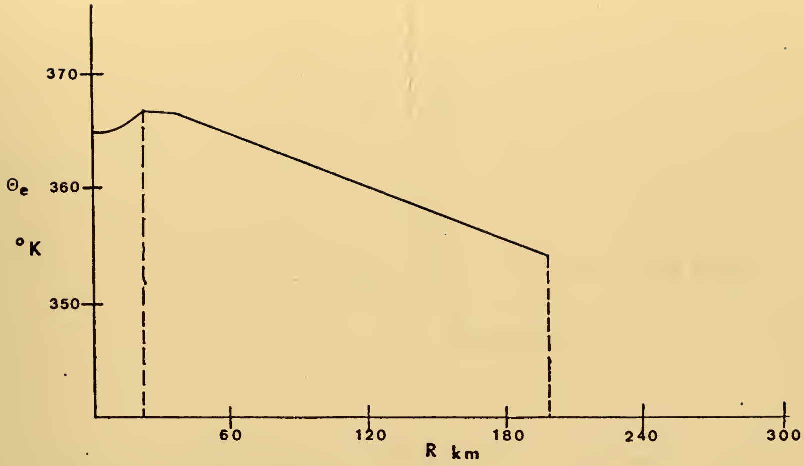


Figure 7. Same as Figure 3 except equivalent potential temperature.

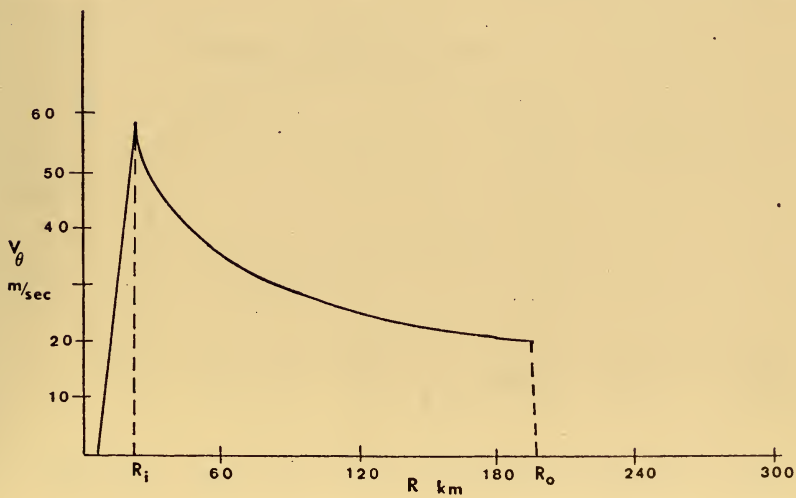


Figure 8. Same as Figure 3 except tangential component of the wind.

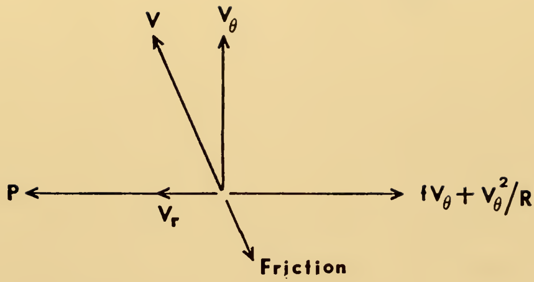


Figure 9. Illustrating the forces acting in the boundary layer of an axisymmetric hurricane.

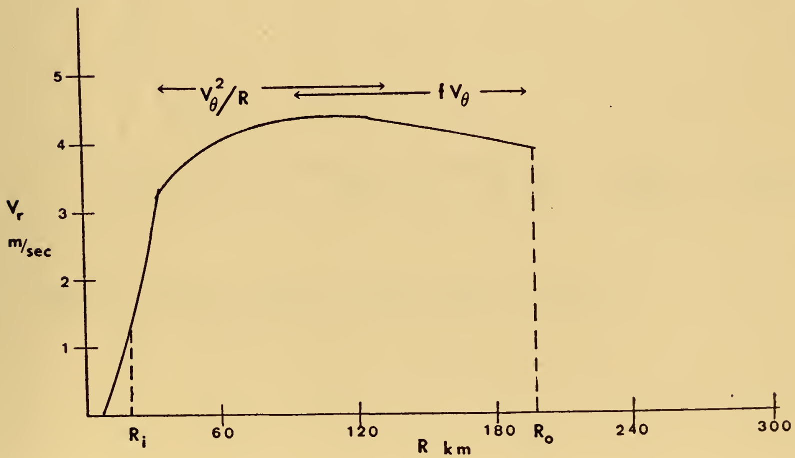


Figure 10. Same as Figure 3 except radial component of the wind.

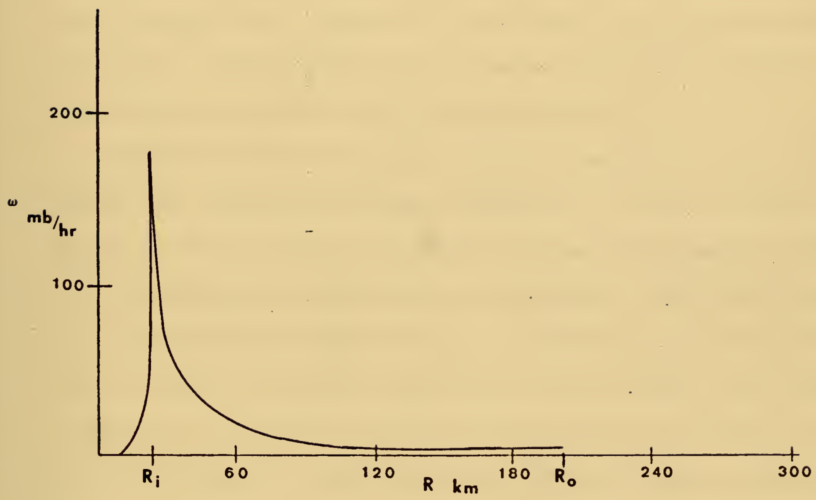


Figure 11. Same as Figure 3 except vertical motion.

through the buoyant energy gain represented by the $\theta_e$ increase from $R_o$ to $R_i$. The convection is sufficient to cause the large pressure gradient which is maintained by the cyclostrophic balance.

Latent heat flux (Figure 12) is dependent on wind speed and the difference in specific humidity of the air and saturated air at the sea-surface temperature (Equation 12). The low moisture content of the air at $R_o$ causes a local maximum in heat flux. The increase in moisture dominates the region from $R_o$ to $3R_i$ causing a decrease in flux despite the increasing wind. Maximum heat flux occurs at $R_i$ where the decrease in pressure and temperature acts to increase the specific humidity difference and the wind reaches a maximum velocity.

Sensible heat flux (Figure 13), which is dependent on wind speed and air-sea temperature difference (Equation 11), reaches a maximum at $R_i$ and is about an order of magnitude less than the latent heat flux.

Precipitation was simulated by two mechanisms. One was the large scale moisture flux through the top of the boundary layer (Figure 14), which reflects the specific humidity and vertical motion. The second mechanism is the removal of moisture which exceeds the critical relative humidity (Figure 15). Both curves are accumulated during the first 15 hours and, therefore, are influenced by the adjustment phase. The peak in Figure 15 at $R_o$ is due to the movement of $R_o$ during adjustment.

1. Experiments with Temperature Variations

In a series of experiments the horizontally uniform water temperature was varied from 28 to 31C while air temperature was initialized at 28C. The radial profiles of the various parameters were similar to those obtained from the base run and illustrated in Figures 3 to 15. There were, however, changes in magnitude and significant values

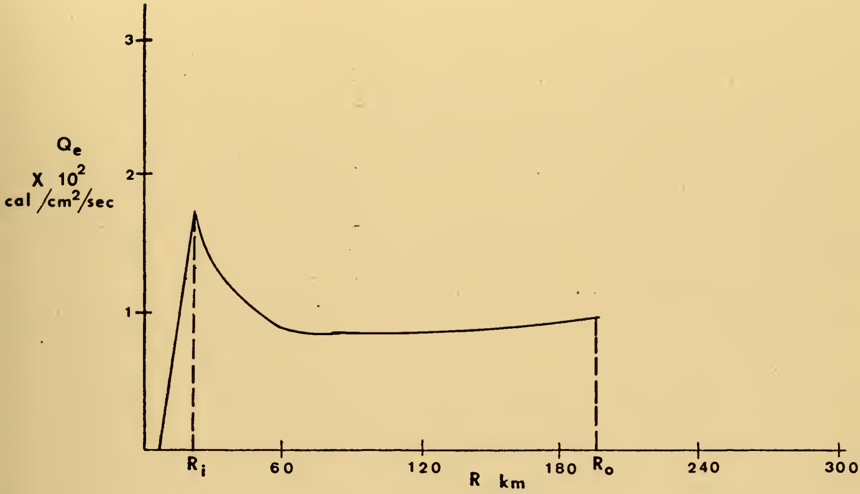


Figure 12. Same as Figure 3 except latent heat flux.

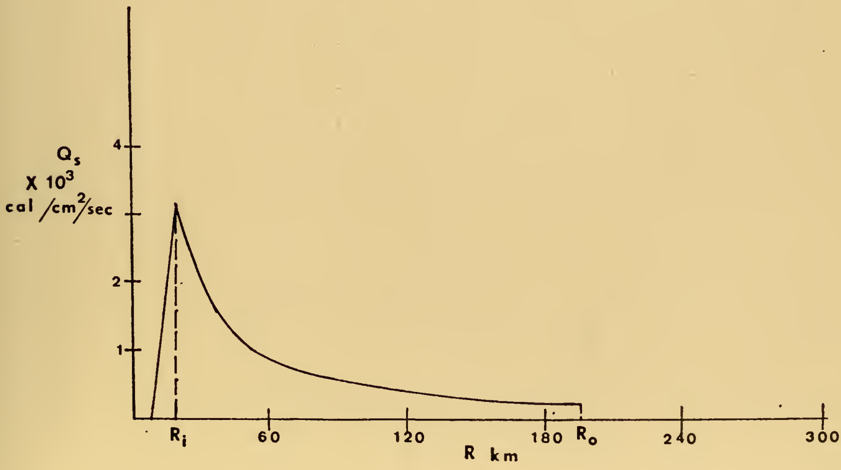


Figure 13. Same as Figure 3 except sensible heat flux.

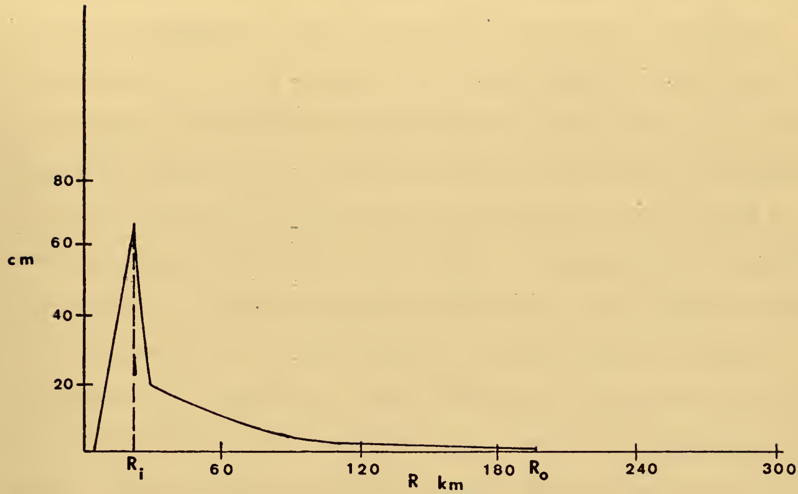


Figure 14. Same as Figure 3 except total moisture flux through the top of the boundary layer for first 15 hours.

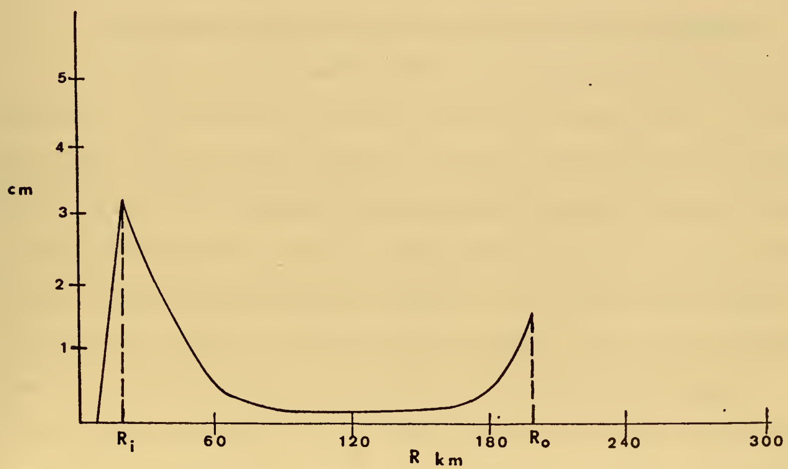


Figure 15. Same as Figure 3 except for total moisture removed by critical relative humidity mechanism for first 15 hours.

are presented in tabular form (Table 1). Air temperature ($T_{a_o}$) at $R_o$ adjusted to within one degree of the water temperature, and the air temperature ($T_{a_i}$) at $R_i$ was about 1.5C cooler than $T_{a_o}$. One of the interesting relationships was the dependence of the model on the difference in $\theta_e$ from $R_o$ to $R_i$. Even when the water temperature was fairly cool, the increase in $\theta_e$ due to air-sea exchange was large enough to sustain hurricane force winds. Since $\theta_{e_o}$ is representative of the ambient values in a tropical atmosphere, and values of 350K are necessary for deep convection, $\theta_{e_o}$ was limited to a minimum value of 350K for determining $V_{\theta_i}$ (Equation 8). This limitation is reflected in the value of $V_{\theta_i}$ for the 28C water temperature case. One of the assumptions of the model is that the energy source for the hurricane is the ocean; therefore, the hurricane should have more energy available and increase in intensity over warmer water. Intensity did increase from 49 m $sec^{-1}$ for the 28C ocean to 62 m $sec^{-1}$ for the 31C ocean.

2. Experiments with Variations of Critical Relative Humidity

Critical relative humidity was used to simulate decreases of moisture in the boundary layer due to convective mechanisms. To test the effect of the critical relative humidity, three profiles were specified (Figure 16). Resulting relative humidity profiles (Figure 17) show that in the convex case relative humidity did not reach critical values except in the eye wall and outer regions. In the concave and linear cases relative humidity reached critical values at all radii between $R_o$ and $R_i$. Latent heat flux is dependent on the difference in vapor pressure of saturated air at sea surface temperature and ambient air; because of this dependence the latent heat flux distribution was affected by the specification of critical relative humidity (Figure 18).

Table I

Significant values in the modified model when the water temperature was varied from 28 to 31C, and air temperature was initialized at 28C.

| $T_w$ ($^oC$) | $T_{a_i}$ ($^oC$) | $T_{a_o}$ ($^oC$) | $\theta_{e_i}$ ($^oK$) | $\theta_{e_o}$ ($^oK$) | $V_{\theta_i}$ (m/sec) | $P_o$ (mbs) |
|---|---|---|---|---|---|---|
| 28 | 26.7 | 27.8 | 359 | 347 | 49 | 975 |
| 29 | 27.0 | 28.5 | 363 | 350 | 57 | 965 |
| 30 | 27.6 | 29.2 | 367 | 353 | 59 | 961 |
| 31 | 28.4 | 29.9 | 371 | 356 | 62 | 958 |

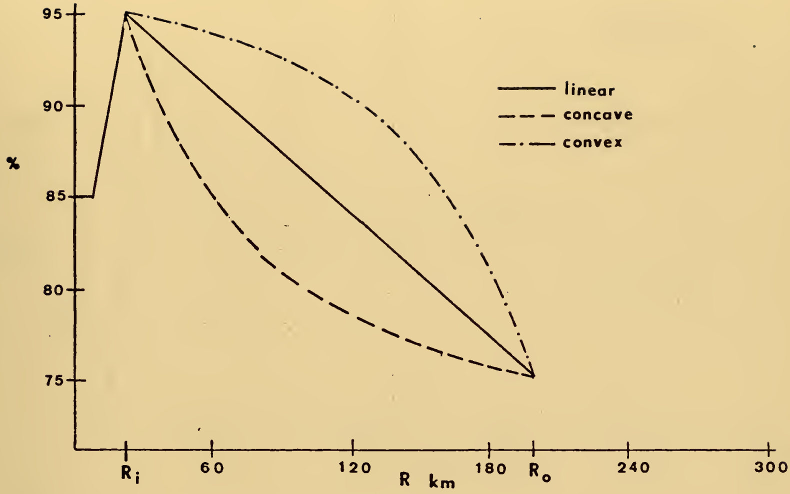


Figure 16. Radial profiles of the three specified critical relative humidity curves.

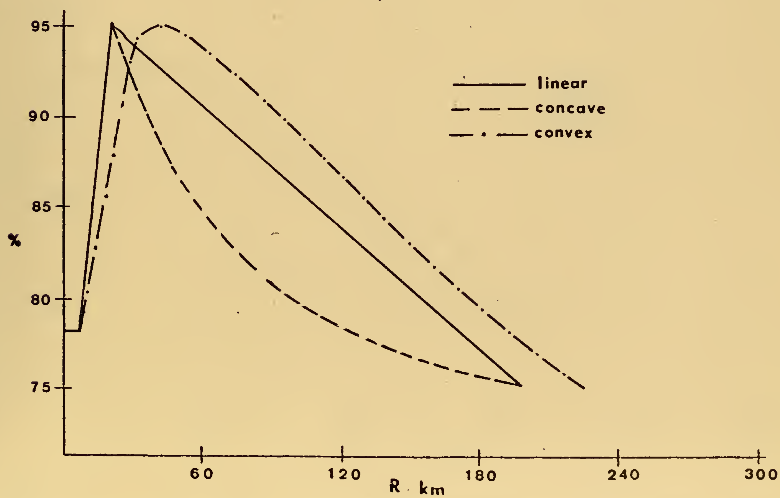


Figure 17. Radial profiles of relative humidity resulting from the three different specifications of critical relative humidity $T_w$ = 30C, $T_a$ initialized at 29C.

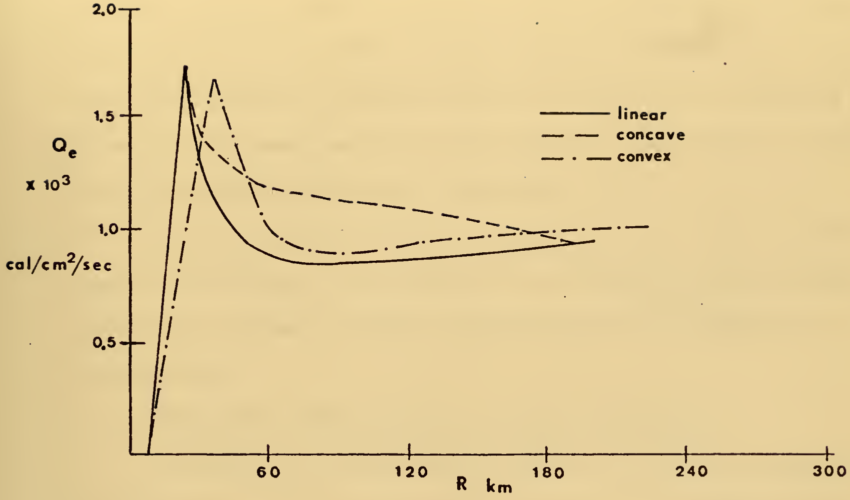


Figure 18. Same as Figure 17 except latent heat flux.

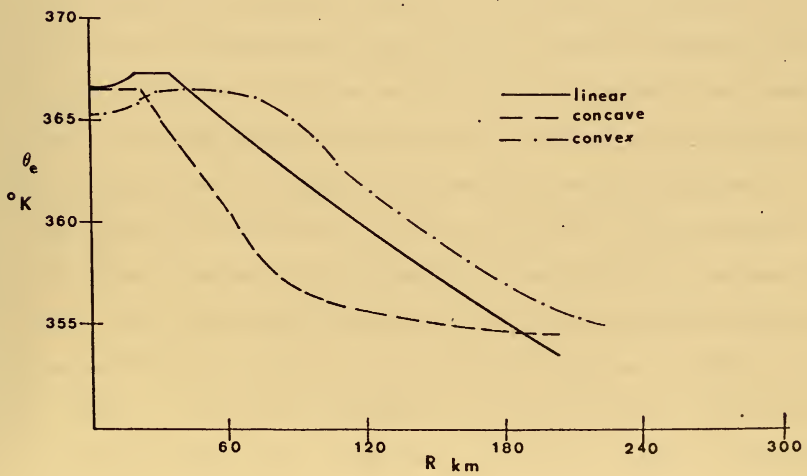


Figure 19. Same as Figure 17 except equivalent potential temperature.

Hurricane intensity, which is determined from $\theta_e$ at $R_o$ and $R_i$, did not vary. The eye wall was made to adjust towards the maximum $\theta_e$; in the convex case maximum $\theta_e$ occurred outside the eye wall and $R_i$ adjusted to 36 km. In the concave and linear cases maximum $\theta_e$ occurred at or inside the eye wall and $R_i$ adjusted to 24 km (Figure 19).

It was concluded that the actual form of the critical relative humidity curve between fixed extrema was not crucial in predicting the intensity of the storm; however, it does affect the distribution of heat exchange.

3. Experiments with Variations of Latent Heat Release

Assuming dry adiabatic expansion in the inflow would result in air temperature in the eye wall region as much as 5 C colder than observed temperatures. Riehl (1954) hypothesized that latent heat release or sensible heat flux, enhanced by blowing spray, must offset the expansion cooling. To simulate the effects of this enhanced heating, the latent heat of condensation of the moisture released to maintain relative humidity below the critical value (Figure 15), was added to the boundary layer. Since the enhanced heating would be a function of the amount of blowing spray, and the amount of blowing spray would be dependent on wind speed, and wind speed is a function of radius, the percentage of heat released was made a linear function of radius with the maximum value at $R_i$, and no latent heat release at $R_o$. Corgnati experimented with releasing 100% of this latent heat at all radii and found a marked increase in intensity. Table II illustrates the effects of latent heat release in the modified model. The increase in $\theta_{e_i}$, while $\theta_{e_o}$ remained unaffected, resulted in an increased intensity.

Table II

Variations of significant values with latent heat released in the boundary layer.

| latent heat release at $R_i$ (%) | $T_{a_i}$ (°C) | $T_{a_o}$ (°C) | $\theta_{e_i}$ (°K) | $\theta_{e_o}$ (°K) | $V_{\theta_i}$ (m/sec) | $P_o$ (mb) |
|---|---|---|---|---|---|---|
| 0 | 27.9 | 29.5 | 367 | 354 | 58 | 963 |
| 25 | 28.3 | 29.5 | 371 | 354 | 69 | 951 |
| 50 | 28.5 | 29.5 | 373 | 354 | 70 | 944 |
| 75 | 28.7 | 29.5 | 375 | 354 | 72 | 941 |
| 100 | 28.6 | 29.6 | 376 | 354 | 74 | 938 |

Although latent heat was used, the heat gain could also be produced by an enhanced sensible heat transfer due to blowing spray. In all probability both latent heat release and enhanced sensible heat transfer play some role in offsetting expansion cooling in the boundary layer. The temperature profile of the model, without latent heat release, was in agreement with observed temperature profiles. The model was therefore run with no latent heat release in the boundary layer.

## B. CARDONE'S BOUNDARY LAYER MODEL

Cardone's two layer baroclinic boundary layer model assumes horizontal homogeneity, stationarity, $K_m$ equal to a constant in the Ekman layer and

$$K_m = kU_* z / \phi_u(z/L') \tag{37}$$

in the surface layer. The model also involves various empirically determined constants based on data from mid-latitudes. Despite these limitations it was felt that a boundary layer based on similarity theory would provide an internally consistent model of an hurricane boundary layer. The inputs to Cardone's model were surface gradient wind, virtual temperature difference between the air in the boundary layer and saturated air at the sea surface temperature, and latitude.

### 1. Application of Cardone's Boundary Layer Model

Several problems arose with the direct application of Cardone's model in place of the bulk transfer equations and the integrated inflow from the tangential wind equation. The model hurricane decayed rapidly during the adjustment phase, and heat and moisture fluxes were well below the 3000 to 5000 cal cm$^{-2}$ day$^{-1}$ values determined by Whitaker (1967) to occur in the hurricane force wind region of hurricane Betsy.

Investigation showed that radial wind (Figure 20), determined from Equations (34) and (35), increased inward from $3R_i$ to $R_i$. Because $V_r$ must go to zero in the eye, vertical motion at the eye wall was on the order of 1500 mb $hr^{-1}$. In this region the vertical transport of moisture exceeded the sum of the horizontal transport and evaporation, which decreased $\theta_{e_i}$ and led to a decrease in intensity. Haltiner and Martin (1957) have shown that the balance of forces in a vortex may be dependent on centrifugal force. This was included in Cardone's model by replacing f by f' as formulated in Equation (31). The time scaling factor then became

$$(f + V_\theta R^{-1})^{-1} , \tag{38}$$

which had the effect of reducing the height of frictional influence as $V_\theta R^{-1}$ increased. In particular, the height of the constant stress layer was reduced from about 50 meters at $R_o$ to about 20 meters at $R_i$ (Figure 21). To maintain consistency within the boundary layer, the centripetal acceleration also had to be included in term B (Equation 36) of the Ekman spiral. The formulation for $V_r$ within the spiral layer became

$$V_r(z) = \sqrt{2}\, e^{-\left(\frac{f + \frac{V_\theta(z)}{R}}{h\, U_* \, k2}\right)^{1/2} z} \sin\alpha \sin\left[\alpha + \frac{3\pi}{4} - \left(\frac{f + \frac{V_\theta(z)}{R}}{h\, U_* \, k2}\right)^{1/2} z\right] \tag{39}$$

where $V_\theta(z)$ is defined by

$$V_\theta(z) = V_\theta + \sqrt{2}\, e^{-\left(\frac{f + \frac{V_\theta(z)}{R}}{h\, U_* \, k2}\right)^{1/2} z} \sin\alpha \cos\left[\alpha + \frac{3\pi}{4}\left(\frac{f + \frac{V_\theta(z)}{R}}{h\, U_* \, k2}\right)^{1/2} z\right] \tag{40}$$

To determine $V_r$ in the spiral layer an iterative technique was employed in determining $V_\theta(z)$ using heights (z) at 10 meter intervals. Then $V_r(z)$ was determined at each height (Figure 22) using the $V_\theta(z)$ for that height.

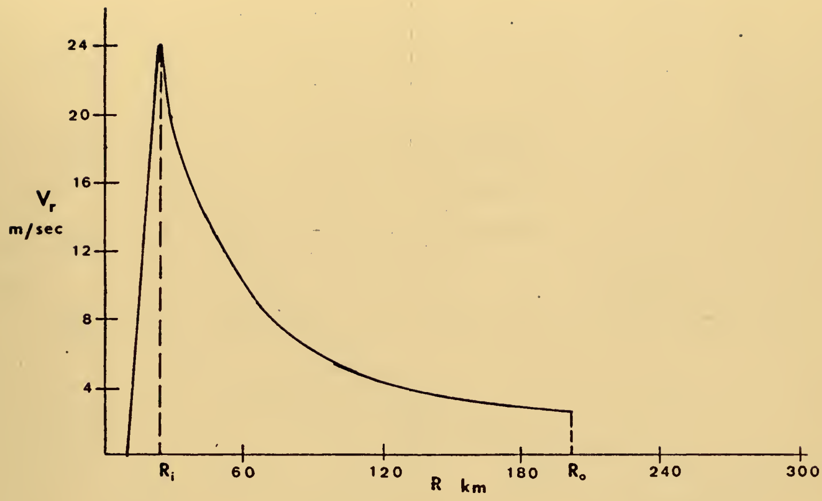


Figure 20. Radial profile of radial component of the wind resulting from direct application of Cardone's boundary layer model.

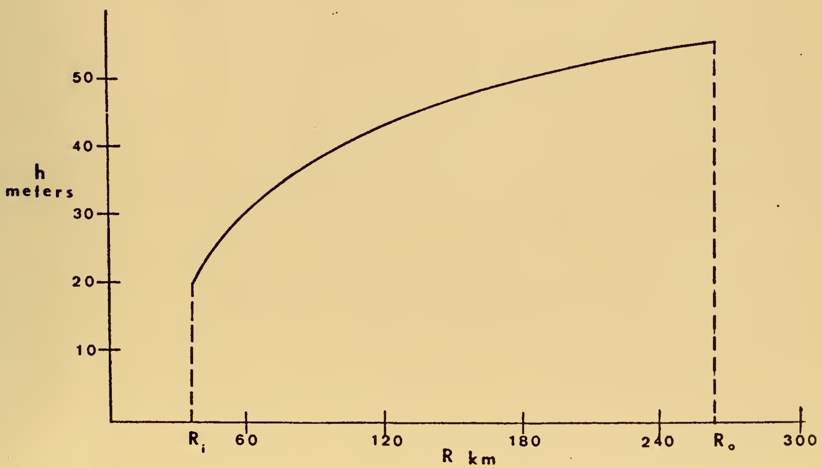


Figure 21. Radial profile of height of the surface layer, illustrating decreasing height of frictional influence due to cyclostrophic flow.

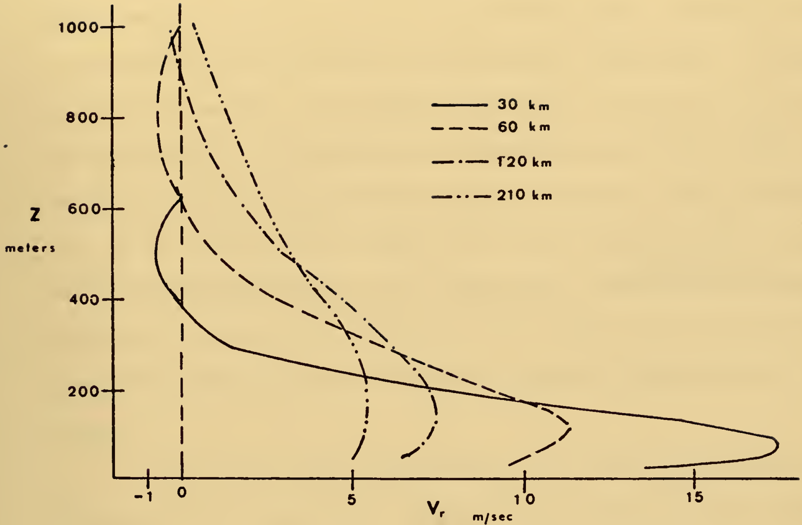


Figure 22. Vertical variation of radial component of the wind in the spiral layer, derived using iterative technique.

The integrated radial wind in the spiral layer was then determined by averaging the values of $V_r(z)$ over the spiral layer. Using an iterative technique proved to be rather time consuming. Because $V_\theta(z)$ increased rapidly with height, the assumption that $V_\theta(z)$ was equal to $V_\theta$ at the top of the boundary layer resulted in integrated values of $V_r(z)$ that closely approximated the averaged values of $V_r(z)$ (Table 3). The assumption that $V_\theta$ was constant with height in the spiral layer was used in determining the integrated value of $V_r$ (Figure 23). Including centrifugal forces was now consistent within the entire model and the rapid decay described earlier, as well as the extreme vertical motion, was no longer evident.

In a study of water temperatures in the wake of hurricane Betsy, Whitaker (1967) estimated the heat flux in the hurricane force wind region to be between .035 and .058 cal cm$^{-2}$ sec$^{-1}$. The application of Cardone's model produced heat fluxes with a maximum value around .02 cal cm$^{-2}$ sec$^{-1}$ (Figure 24). One of the assumptions in Cardone's model was that the ratio of the turbulent transfer coefficient for heat ($K_h$) to turbulent transfer coefficient for momentum ($K_m$) was unity. Businger et al (1971) found "The ratio of the eddy diffusivities ($a_h$) for heat and moisture is greater than unity. The value at neutral is 1.35; and shows a marked increase with instability." Since heat transfer, as determined in the model, is directly dependent on $a_h$ (Equation 32), increasing $a_h$ increased the heat flux. In a hurricane the large quantity of blowing spray should serve to enhance the heat transfer. Furthermore, the velocity imparted to this blowing spray should serve to increase the momentum transfer. To simulate the increasing heat flux and momentum transfer, the roughness length ($Z_o$) was increased by increasing the

Table III

Comparison of integrated $V_r$ values obtained using iterative technique, and assuming $V_\theta(z)$ constant.

| Radius (km) | 30 | 60 | 90 | 120 | 150 | 180 | 210 |
|---|---|---|---|---|---|---|---|
| $V_r$ (m/sec) iterative technique | 3.14 | 3.22 | 3.42 | 3.49 | 3.40 | 3.38 | 3.20 |
| $V_r$ (m/sec) $V_\theta(z)$ const | 3.22 | 3.27 | 3.47 | 3.53 | 3.43 | 3.40 | 3.21 |

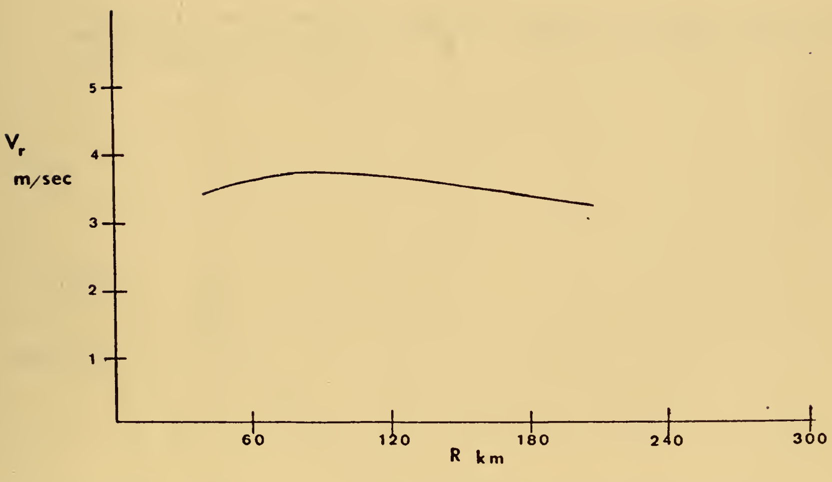


Figure 23. Radial profile of integrated radial component of the wind assuming cyclostrophic flow and $V_\theta$ constant within the spiral layer.

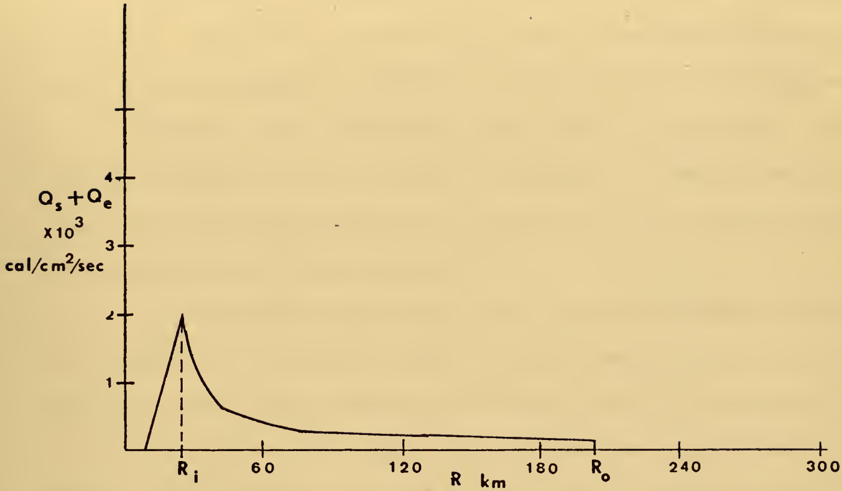


Figure 24. Radial profile of combined sensible and latent heat flux obtained using Cardone's model, $C_2$ = .00428, $a_h$ = 1.0, $T_w$ = 30C, and $T_a$ initialized at 29C.

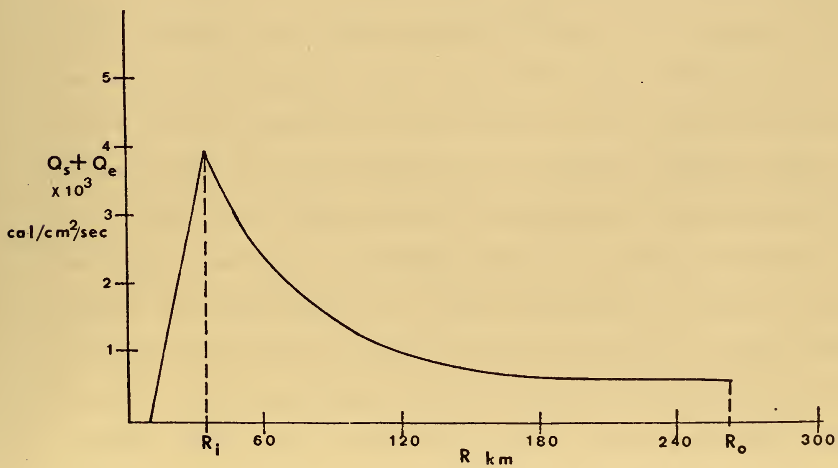


Figure 25. Same as Figure 24 except $a_h$ = 2.0, $C_2$ = .05.

the coefficient ($C_2$) of the $U_*^2$ term in Cardone's formulation of $Z_o$ (Equation 29). It was found that realistic values of heat flux were obtained when $C_2$ was increased from .00428 to .05, and $a_h$ taken as 2.0 (Figure 25).

Cardone's model, with cyclostrophic flow, $C_2$ increased to .05, and $a_h$ increased to 2, was now used to determine the sensible and latent heat fluxes, replacing Equations (11) and (12), and the average radial wind component, replacing Equation (6).

A base run was made in which water temperature was set at 30C, air temperature initialized at 29C, critical relative humidity set at 95% at $R_i$ with a linear decrease to 75% at $R_o$, and no latent heat released within the boundary layer. This base run was compared to the base run illustrated by Figures 3 through 15 and discussed earlier. Cardone's model produced greater latent and sensible heat flux (Figures 12 and 25) which led to slightly warmer temperatures at $R_i$ and increased $\theta_{e_i}$. As a result of the increased $\theta_{e_i}$, $V_{\theta_i}$ was about 5 m sec$^{-1}$ greater. Table 4 compares some of the significant values of the base runs. The use of Cardone's boundary layer model provided some additional parameters that were indicative of the structure of the boundary layer, as illustrated in Figures 26 through 29. The modified stability length (L'), illustrated in Figure 26, can be interpreted to be proportional to the ratio of mechanical and buoyant production of turbulent kinetic energy. The large increase of L', with increasing $V_\theta$, reflects an increase in the mechanical versus the buoyant production of kinetic energy. Surface stress values (Figure 27), which increases rather dramatically to a maximum value at $R_i$, are in close agreement with stress values deduced by Miller (1962) using data from hurricane Helene (Table 5). The increase in stress towards the center is due to the increase in wind and the

Table IV

Comparison of significant values obtained from two base runs.

| parameter | Corgnati's modified model | Cardone's model |
|---|---|---|
| $V_{\theta_i}$ (m/sec) | 58 | 62 |
| $T_{a_i}$ ($^oC$) | 27.9 | 28.0 |
| $T_{a_o}$ ($^oC$) | 29.5 | 29.2 |
| $\theta_{e_i} - \theta_{e_o}$ ($^oK$) | 13 | 15 |
| $P_o$ (mbs) | 963 | 953 |

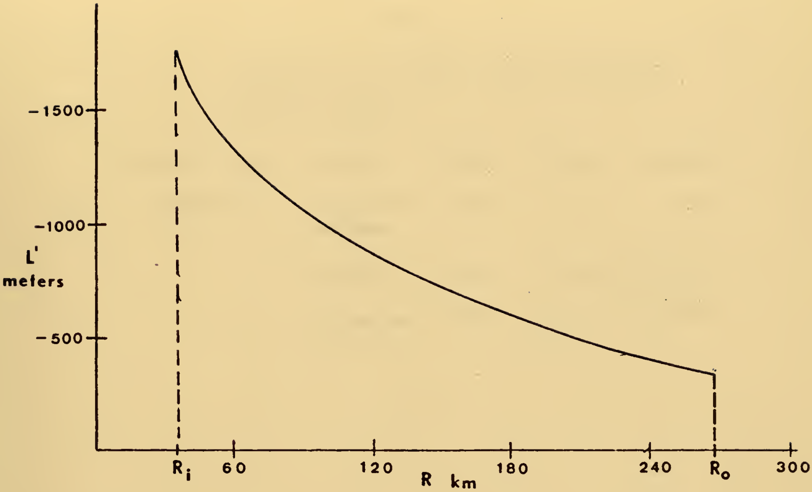


Figure 26. Same as Figure 25 except modified stability length.

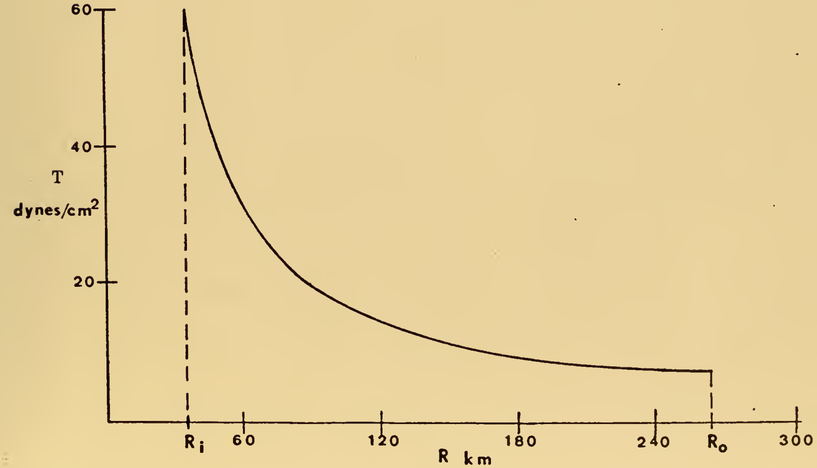


Figure 27. Same as Figure 25 except surface stress.

Table V

Comparison of surface stress determined by Miller, and values obtained from the hurricane model.

| surface stress | Radius | 0-20nm | 20-40nm | 40-60nm |
|---|---|---|---|---|
| dynes/cm$^2$ | Miller's values | 60.0 | 51.0 | 27.6 |
| | Radius | 20nm | 30nm | 50nm |
| | computed | 60 | 35 | 20 |

rougher surface. The increase of stress with decreasing radial distance is reflected in the increase in inflow angle within the constant stress layer (Figure 28); also in the radial velocity at the top of the surface layer (Figure 29). These values are comparable to inflow angles and radial velocities observed in actual hurricanes. One of the assumptions made in Corgnati's model was that the cosine of the inflow angle could be closely approximated by unity. Despite the increase in the inflow angle, this appears to be a good approximation.

2. Temperature Experiments with Cardone's Model

To further test the use of Cardone's boundary layer model, experiments were conducted in which water temperature was varied from 28 to 31C. These experiments were similar to the ones conducted with Corgnati's modified model, and discussed in section IIIA1. The heat flux distribution obtained, using Cardone's model, appeared to be more sensitive to temperature variations than the heat flux distribution obtained using the bulk aerodynamic transfer formulas (Figure 30). Due to the differing heat flux, the variation in the difference between extrema values of $\theta_e$ was greater, using Cardone's model, than the variations obtained using bulk aerodynamic transfer formulas. The result of these greater variations was that, using Cardone's model, a sea surface temperature increase from 28 to 31C produced a $V_{\theta_i}$ increase of 25 m sec$^{-1}$ (Table 6); while using bulk aerodynamic transfer formulas, the same temperature increase produced only a 13 m sec$^{-1}$ increase in $V_{\theta_i}$. It was felt that the greater sensitivity to sea surface temperature, exhibited by Cardone's boundary layer model, more closely simulated the dependence of a hurricane on the oceanic heat source.

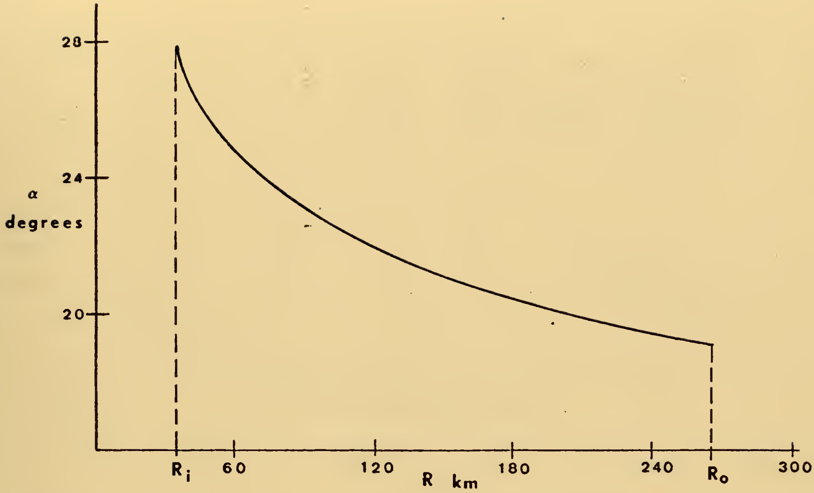


Figure 28. Same as Figure 25 except inflow angle in surface layer.

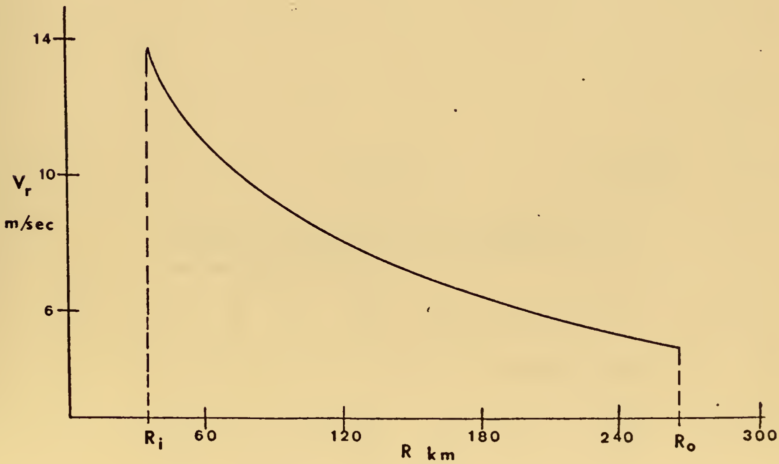


Figure 29. Same as Figure 25 except radial component of the wind at top of surface layer.

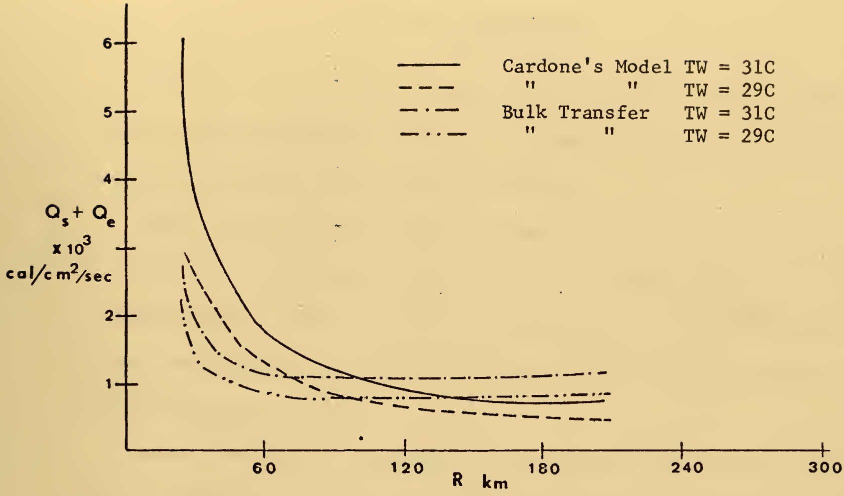


Figure 30. Radial profiles of combined latent and sensible heat flux, comparing values obtained from Cardone's model with $T_w$ = 31C and $T_w$ = 29C, and Corgnati's modified model with $T_w$ = 31C and $T_w$ = 29C, $T_a$ initialized at 28C.

Table VI

Changes in significant values due to varying water temperature, air temperature initialized at 28C.

| $T_w$ ($^oC$) | $T_{a_i}$ ($^oC$) | $T_{a_o}$ ($^oC$) | $\theta_{e_i}$ ($^oK$) | $\theta_{e_o}$ ($^oK$) | $V_{\theta_i}$ (m/sec) | $P_o$ (mb) |
|---|---|---|---|---|---|---|
| 28 | 27.1 | 28.0 | 358 | 348 | 45 | 979 |
| 29 | 27.2 | 28.2 | 363 | 349 | 58 | 960 |
| 30 | 27.8 | 28.7 | 368 | 351 | 66 | 952 |
| 31 | 28.5 | 29.3 | 373 | 353 | 70 | 944 |

## IV. CONCLUSIONS

The results of this study have indicated that a marine boundary layer based on similarity theory can be applied to an hurricane and improve the effects of air-sea interaction.

First, results indicate that the time scaling factor in cyclostrophic flow is dependent on $(f + V_\theta R^{-1})^{-1}$, rather than f as in Cardone's model. The effect of the centripetal acceleration was to reduce the height of frictional influence as wind speed increased and radial distance decreased.

Second, observed temperature fields indicate that enhanced heat flux is necessary to offset the adiabatic expansion cooling within the boundary layer of an hurricane. This enhanced heat flux is likely to be due to the large quantities of blowing spray observed in an hurricane. Consequently, the ratio of the coefficients of heat diffusivity to momentum diffusivity was increased from unity to 2. Increasing the roughness length, as a function of friction velocity squared, was used to simulate the increased momentum transfer and resulted in surface stress values that appear to be realistic. The increase in roughness length was further justified by resultant heat flux values that were in agreement with determined values.

Third, the removal of moisture from the boundary layer, through convective mechanisms, appears to have a strong influence on air-sea interaction. Vertical advection by the mean motion is not sufficient to export the large horizontal flux of moisture within the boundary layer and the evaporation. The removal of moisture in excess of a

critical relative humidity value appears to adequately simulate "hot tower" convection and surrounding subsidence.

Finally, in the earlier model of Corgnati (1971) it had been necessary to specify a drag coefficient and extrapolate a surface wind to determine air-sea interaction. However, the external parameters required to use similarity theory were surface gradient wind, and the virtual temperature difference between saturated air at the sea surface temperature, and the air in the boundary layer. The vertical structure of the wind and an implied drag coefficient were inherent in the iterative solution based on similarity theory.

The more complete boundary layer specification based on similarity theory appears to be justified in view of the good agreement obtained between predicted and observed or estimated values of radial inflow, heat flux, and surface stress. Furthermore, the boundary layer model calculates wind profiles within the surface layer, as well as surface stress; and effects of both stability and changes of surface roughness on air-sea interaction have been included in the hurricane model.

One of the assumptions made in this study was that the stability length was defined by density stratification based on virtual temperature. This assumption was crucial in the determination of latent heat flux.

Further studies, in the area of air-sea interaction under high wind speed conditions, are necessary to provide guidance in the selection of empirical constants in the similarity solution. Specifically, the effects of blowing spray, in enhancing heat flux and momentum transfer, may be important in maintaining tropical cyclones.

## BIBLIOGRAPHY


1. Blackadar, A. K., 1965: A simplified two-layer model of the baroclinic neutral atmosphere boundary layer. Air Force Cambridge Research Laboratories Report 65-531, pp. 49-65.

2. Businger, J. P., J. C. Wyngaard, U. Izumi, and E. E. Bradley, 1971: Flux-profile relationships in the atmospheric surface layer. J. Atmos. Sci., 28, 181-189.

3. Cardone, V. J., 1969: Specification of the wind distribution in the marine boundary layer for wave forecasting. New York University, School of Engineering and Science, Scientific Report GSL-TR69-1, University Heights, New York.

4. Charnock, H., 1955: Wind stress on a water surface. Quart. J. Roy. Meteor. Soc., 81, 639.

5. Corgnati, L. B., 1971: Experiments with a simple hurricane-interacting ocean model, M.S. Thesis, Naval Postgraduate School, Monterey.

6. Deppermann, C. E., 1939: Some characteristics of Philippine typhoons. Manila, Bureau of Printing, 143.

7. Haltiner, G. J., F. L. Martin, 1957: Dynamical and Physical Meteorology. New York, McGraw-Hill Book Co., 181-183, 234-241.

8. Lettau, H. H., 1959: Wind profile, surface stress and geostrophic drag coefficients in the atmospheric surface layer. Advances in Geophysics, 6, 241-257.

9. McConathy, D. R., 1972: Specification of marine surface boundary layer parameters, M.S. Thesis, Naval Postgraduate School, Monterey.

10. Miller, B. I., 1962: On the momentum and energy balance of hurricane Helene (1958). National Hurricane Research Project Report No. 53, 10-13.

11. Panofsky, H. A., 1963: Determination of stress from wind and temperature measurements. Quart. J. Roy. Meteor. Soc., 88, 85-94.

12. Riehl, H., 1954: Tropical Meteorology. New York, McGraw-Hill Book Co., 281-356.

13. Riehl, H., and J. S. Malkus, 1961: Some aspects of hurricane "Daisy", 1958. Tellus 13, 181, 213.

14. Riehl, H., 1963: Some relations between wind and thermal structure of steady-state hurricanes. J. Atmos. Sci., 20, 276-287.

15. Robinson, G. D., 1966: Another look at some problems of the air-sea interface. Quart. J. Roy. Meteor. Soc., 92, 451-465.

16. Shea, D. J., 1972: The structure and dynamics of the hurricanes inner core region. Department of Atmospheric Science, Colorado State University, Atmospheric Science Paper No. 182, Fort Collins, 134.

17. Whitaker, W. D., 1967: Quantitative determination of heat transfer from sea to air during passage of hurricane Betsy, M.S. Thesis, Graduate College of the Texas A&M University, 65, 28.

INITIAL DISTRIBUTION LIST

| | | No. Copies |
|---|---|---|
| 1. | Defense Documentation Center<br>Cameron Station<br>Alexandria, Virginia 22314 | 2 |
| 2. | Library, Code 0212<br>Naval Postgraduate School<br>Monterey, California 93940 | 2 |
| 3. | Professor R. L. Elsberry, Code 51Es<br>Department of Meteorology<br>Naval Postgraduate School<br>Monterey, California 93940 | 8 |
| 4. | Professor D. F. Leipper<br>Department of Oceanography<br>Naval Postgraduate School<br>Monterey, California 93940 | 1 |
| 5. | Lieutenant Commander N. A. S. Pearson<br>Helicopter Support Squadron Seven<br>Naval Air Station Imperial Beach<br>Imperial Beach, California 92032 | 2 |
| 6. | Naval Weather Service Command<br>Naval Weather Service Command Headquarters<br>Washington Navy Yard<br>Washington, D. C. 20390 | 1 |
| 7. | Lieutenant Commander R. W. Lyons<br>Fleet Weather Central<br>Norfolk, Virginia 23511 | 1 |
| 8. | Professor K. L. Davidson, Code 51Ds<br>Department of Meteorology<br>Naval Postgraduate School<br>Monterey, California 93940 | 1 |
| 9. | Professor R. L. Haney, Code 51Hy<br>Department of Meteorology<br>Naval Postgraduate School<br>Monterey, California 93940 | 1 |
| 10. | Professor R. J. Renard, Code 51Rd<br>Department of Meteorology<br>Naval Postgraduate School<br>Monterey, California 93940 | 1 |

Security Classification

# DOCUMENT CONTROL DATA - R & D

*(Security classification of title, body of abstract and indexing annotation must be entered when the overall report is classified)*

| | |
|---|---|
| 1. ORIGINATING ACTIVITY *(Corporate author)*<br>Naval Postgraduate School<br>Monterey, California 93940 | 2a. REPORT SECURITY CLASSIFICATION<br>Unclassified<br>2b. GROUP |

3. REPORT TITLE

Further Experiments with an Hurricane-Ocean Interaction Model

4. DESCRIPTIVE NOTES *(Type of report and, inclusive dates)*

Master's Thesis; September 1972

5. AUTHOR(S) *(First name, middle initial, last name)*

Nils A. S. Pearson

| 6. REPORT DATE | 7a. TOTAL NO. OF PAGES | 7b. NO. OF REFS |
|---|---|---|
| September 1972 | 60 | 17 |

| | |
|---|---|
| 8a. CONTRACT OR GRANT NO. | 9a. ORIGINATOR'S REPORT NUMBER(S) |
| b. PROJECT NO. | |
| c. | 9b. OTHER REPORT NO(S) *(Any other numbers that may be assigned this report)* |
| d. | |

10. DISTRIBUTION STATEMENT

Approved for public release; distribution unlimited.

| | |
|---|---|
| 11. SUPPLEMENTARY NOTES | 12. SPONSORING MILITARY ACTIVITY<br>Naval Postgraduate School<br>Monterey, California 93940 |

13. ABSTRACT

Modifications were made to Corgnati's (1971) steady state, symmetrical hurricane model, which was based on a model proposed by Riehl (1963), and in which bulk aerodynamic transfer formulas were used to predict the air-sea interaction below a specified vortex. The modifications resulted in a more flexible model in which hurricane intensity was controlled by sensible and latent heat fluxes, which were in turn dependent on the ocean surface temperature. A boundary layer model based on similarity theory was then used, to specify air-sea interaction, by replacing the bulk transfer formulas with Cardone's(1969) extension of Blackadar's (1965) two-layer neutral, baroclinic boundary layer model. To achieve realistic results the time scale was modified to include centripetal acceleration, which resulted in a decreasing height of frictional influence with decreasing radius. Varying Cardone's formulation of roughness length and the ratio of eddy exchange coefficients for heat and moisture resulted in stress and heat flux values in agreement with values determined from hurricane observations. Including the complete boundary layer model resulted in greater sensitivity to ocean temperature variations than when bulk transfer formulas were used to determine the air-sea interaction.

| 14. KEY WORDS | LINK A | | LINK B | | LINK C | |
|---|---|---|---|---|---|---|
| | ROLE | WT | ROLE | WT | ROLE | WT |
| Air-sea interaction | | | | | | |
| Hurricane model | | | | | | |
| Boundary layer | | | | | | |
| Latent heat release | | | | | | |
| Sensible heat flux | | | | | | |

Thesis 138060
P316 Pearson
c.1 Further experiments
with an hurricane-ocean
interaction model.